Analysis of EM Scattering from 3D Bi-Anisotropic Objects above a Lossy Half Space Using FE-BI with UV Method

J. Zhu [1], M. M. Li [2], Z. H. Fan [2], and R. S. Chen [2]

[1] College of Communications and Information Engineering
Nanjing University of Posts and Telecommunications, Nanjing, 210006, China
zhujian82@njupt.edu.cn

[2] Department of Communication Engineering
Nanjing University of Science and Technology, Nanjing 210094, China
eechenrs@mail.njust.edu.cn

Abstract ─ In this paper, the finite-element boundary integral (FE-BI) method with UV method is applied to analyze the electromagnetic scattering from arbitrary three-dimensional bi-anisotropic objects located above a lossy half space. The form of electric field in bi-anisotropic materials is provided and cast into linear equations by finite element method (FEM), which is valid for any complex materials. The boundary integral equation (BI) is used to truncate the computational domain by using a half-space dyadic Green's function via the discrete complex image method (DCIM). A fast numerical approach, the UV method, is employed to decrease the memory requirement and the total CPU time for FE-BI solution. Numerical results are carried out so as to validate our developed algorithm. Further, the effects of different material parameters on the scattering characteristics of typical bi-anisotropic object in half space are examined and compared.

Index Terms - Bi-anisotropic media, electro-magnetic scattering, FE-BI, half-space, and UV method.

I. INTRODUCTION

Artificial microwave complex materials, including isotropic/bi-isotropic, anisotropic/bi-anisotropic media, have been many potential applications in the fields of antennas, alteration of the radar cross sections, since the media parameter provides an extra degree of freedom to control the scattering properties of targets [1-2].

Many numerical techniques have been extensively studied for investigation of electromagnetic scattering from complex material objects in free space, such as the finite difference time domain method (FDTD) [3], the finite element method (FEM) [4], the method of moment (MoM) [5-7], the volume-surface integral equation (VSIE) [8] and the hybrid finite-element boundary integral method (FE-BI) [9]. However, to the best of our knowledge, very few works are directly related to the applications of numerical methods to investigate complex material objects located above a lossy half space, especially containing the bi-anisotropic media. FDTD and FEM based on differential equation are very flexible in terms of material geometry and composition. However, they are vulnerable to the impact of boundary truncation for scattering analysis [11]. MoM is the most popular approach, which has been developed for the electromagnetic scattering by a 3-D chiral object in the presence of a lossy half space [12, 13]. However, MoM is still quite cumbersome to be applied to the case of strongly inhomogeneous dielectric objects. Moreover, this method relies on the closed-form Green's functions, which are very difficult to obtain for general bi-anisotropic media [12].

The hybrid method FE-BI is well known as a powerful tool to solve the complex scattering problems [9, 10, 14], which deals with the inside fields via FEM flexibly and applies boundary integral equation with an appropriate Green's

Submitted On: Sept. 3, 2012
Accepted On: Oct. 31, 2013

function to truncate the computational domain for the unbounded domain. In this paper, FE-BI has been extended to study electromagnetic scattering from arbitrary bi-anisotropic objects located above a lossy half space. In the boundary integral formulations, one of the most complicated issues is evaluation of the half-space dyadic Green's function [12, 13, 17-20]. Each component of the dyadic is represented in general via a Sommerfield integral (SI), the direct numerical evaluation of which makes a MoM analysis prohibitive. The numerical integration of SI is time consuming since the integrand is both highly oscillating and slowly decaying. Therefore, the discrete complex image method (DCIM) [15] is employed to overcome this difficulty.

However, the final FE-BI system of equations consists of a partly-full, partly-sparse matrix, the equation of that is difficult to solve efficiently for iterative methods. Fortunately, the difficulty can be overcome by use of the fast multipole method (FMM) [16]. In [12, 13, 17, 18], FMM has been extended for general targets in the presence of a lossy half space. The "far" terms are evaluated via an approximation to the dyadic Green's function, using a single appropriately weighted image in the real space [17]. However, this real-image representation of the Green's function is appropriate for expansion when the source and observation points are separated by a wavelength or more [16]. This determines the large minimum group size of the FMM, which leads to a low efficiency. In this paper, the rank-based methods, the multilevel UV method [21] is applied to overcome the above difficulty for the approximation to the half-space Green's function in the "far" terms. The computational complexity and memory requirement of the multilevel UV method is $O(rN\log N)$, where r is the typical rank at the largest level [21]. The multilevel UV method is the impedance matrix decomposition based method and kernel function independent. The half-space Green's function in the "far" terms is evaluated via DCIM, and the multilevel UV method needs only to deal with the final low-ranked far matrix. Thus, the approximation error is controllable via the threshold in the UV matrix compression [21]. The multilevel UV method is easy to be applied in the existing FE-BI code without large change of the algorithms.

The paper is organized as follows. The formulation employed to solve the problem is reported in section II, together with an introduction of the multilevel UV method for FE-BI analysis. In section III, numerical results are carried out so as to validate our developed algorithm. The final remarks are included in section IV.

II. FORMULATION

An arbitrary complex media object above a half space is considered. The relative permittivity and permeability of the object and the lower half-space are denoted by $(\overline{\overline{\varepsilon}}, \overline{\overline{\mu}}, \overline{\overline{\xi}}, \overline{\overline{\zeta}})$ and $(\varepsilon_{gr}, \mu_{gr})$. FEM is used to describe the electric field in volume V. A boundary integral equation about the equivalent electric current **J** and magnetic current **M** on the surface of the object is solved by MoM to complement FEM equations.

A. Weak form of wave equation in complex media

The electric and magnetic fields **E** and **H** radiated by the surface current **J** and **M** in an unbounded bi-anisotropic media are governed by the following constitutive relations [4, 10],

$$\begin{aligned} \mathbf{D} &= \overline{\overline{\varepsilon}} \bullet \mathbf{E} + \overline{\overline{\xi}} \bullet \mathbf{H} \\ \mathbf{B} &= \overline{\overline{\zeta}} \bullet \mathbf{E} + \overline{\overline{\mu}} \bullet \mathbf{H}, \end{aligned} \tag{1}$$

where $\overline{\overline{\varepsilon}}$ and $\overline{\overline{\mu}}$ are the permittivity and permeability tensors, respectively. $\overline{\overline{\xi}}$ and $\overline{\overline{\zeta}}$ are the tensors describing the magnetoelectric coupling effects in bi-anisotropic media. The wave equation has the following equation,

$$\mathcal{L} \bullet \mathbf{E} = -j\omega \mathbf{J}_i \tag{2}$$

where $\mathcal{L} = \left(-\nabla + j\omega\overline{\overline{\xi}}\right) \bullet \overline{\overline{\mu}}^{-1} \bullet \left(\nabla + j\omega\overline{\overline{\zeta}}\right) + \omega^2 \overline{\overline{\varepsilon}}$.

By taking the inner product with test functions E^a both sides of equation (2), then we have the following weak form of vector electric wave equation,

$$\begin{aligned} F\left(\mathbf{E}, \mathbf{E}^a\right) = & < \mu^{-1} \bullet \left(\nabla \times \mathbf{E}^a + j\omega\overline{\overline{\xi}} \bullet \mathbf{E}^a\right), \nabla \times \mathbf{E} + j\omega\overline{\overline{\zeta}} \bullet \mathbf{E} > \\ & + \omega^2 < \mathbf{E}^a, \overline{\overline{\varepsilon}} \bullet \mathbf{E} > - < \mathbf{E}^a, j\omega \mathbf{J}_i > - < j\omega \mathbf{J}_i{}^a, \mathbf{E} > \\ & - j\omega \int \left(\hat{n} \times \mathbf{E}^a\right)^* \bullet \mathbf{H}^{ext} dS. \end{aligned} \tag{3}$$

B. Half-space boundary integral formulation

The electric and magnetic fields outside S can be calculated by the surface boundary integral at the

surface S. As a scatterer, this object is illuminated by a total "incident field" including two components, one is the incident field ($\boldsymbol{E}^{inc}, \boldsymbol{H}^{inc}$) and the other is the reflected field ($\boldsymbol{E}^{ref}, \boldsymbol{H}^{ref}$) in the presence of the half space. The combined-field integral equation (CFIE) is used as follows,

$$\begin{aligned}\hat{t}\cdot\left(\mathbf{E}^{inc}(\mathbf{r})+\mathbf{E}^{ref}(\mathbf{r})\right)=\hat{t}\cdot[&\frac{1}{2}\mathbf{E}(\mathbf{r})+jk_0\iint_S \overline{\overline{\mathbf{K}}}_{ii}^{A}(\mathbf{r},\mathbf{r}')\cdot\mathbf{J}_S(\mathbf{r}')dS'\\&+\frac{j}{k_0}\oiint_S \nabla'\cdot\mathbf{J}_S(\mathbf{r}')\nabla K_{ii}^{\phi e}(\mathbf{r},\mathbf{r}')dS'\\&+\iint_S \nabla\times\overline{\overline{\mathbf{G}}}_{ii}^{F}(\mathbf{r},\mathbf{r}')\cdot\mathbf{M}_S(\mathbf{r},\mathbf{r}')dS'],\end{aligned} \tag{4}$$

$$\begin{aligned}\hat{n}\times\left(\overline{\mathbf{H}}^{inc}(\mathbf{r})+\overline{\mathbf{H}}^{ref}(\mathbf{r})\right)=\hat{n}\times[&\frac{1}{2}\overline{\mathbf{H}}(\mathbf{r})+jk_0\iint_S \overline{\overline{\mathbf{K}}}_{ii}^{F}(\mathbf{r},\mathbf{r}')\cdot\mathbf{M}_S(\mathbf{r}')dS'\\&+\frac{j}{k_0}\oiint_S \nabla'\cdot\mathbf{M}_S(\mathbf{r}')\nabla K_{ii}^{\phi m}(\mathbf{r},\mathbf{r}')dS'\\&-\iint_S \nabla\times\overline{\overline{\mathbf{G}}}_{ii}^{A}(\mathbf{r},\mathbf{r}')\cdot\mathbf{J}_S(\mathbf{r},\mathbf{r}')dS'],\end{aligned} \tag{5}$$

where $\mathbf{J}_S=\eta\hat{n}\times\mathbf{H}$ and $\mathbf{M}_S=\mathbf{E}\times\hat{n}$ are the electric current and the equivalent magnetic current over the surface S, respectively. $\overline{\overline{\mathbf{K}}}_{ii}^{A}, \overline{\overline{\mathbf{G}}}_{ii}^{F}, \overline{\overline{\mathbf{K}}}_{ii}^{F}, \overline{\overline{\mathbf{G}}}_{ii}^{A}$ and $K_{ii}^{\phi e}$ and $K_{ii}^{\phi m}$ are the dyadic and the scalar Green's functions for the half-space region, which can be evaluated efficiently via the complex-image technique [15].

RWG [22] and Whitney basis functions [23] are used to expand the current and electric field. Combining equations (3) to (5), the final FE-BI matrix equation is obtained,

$$\begin{bmatrix}K_{II} & K_{IS} & 0\\ K_{SI} & K_{SS} & B\\ 0 & P & Q\end{bmatrix}\begin{Bmatrix}E_I\\ E_S\\ J_S\end{Bmatrix}=\begin{Bmatrix}0\\ 0\\ b\end{Bmatrix} \tag{6}$$

where $\{E_i\}$ is a vector containing the discrete electric field inside V, $\{E_S\}$, and $\{J_S\}$ are vectors containing the discrete electric and current on S, respectively, and finally K_{II}, K_{IS}, K_{SI}, K_{SS}, and B denote the corresponding highly sparse FEM matrices, and {b} is a vector related to the incident field.

C. The multilevel UV method

The dense matrices [P] and [Q] generated by BI equation, which is a bottleneck of the FE-BI method that severely limits the capability of the FE-BI method in dealing with large objects. However, with the discrete complex image, the half-space Green function can be expanded to the exponential form, and then the half-space Green function varies smoothly with distance. Therefore, by grouping with the octree structure, similar to [18, 21], the dense matrices [P] and [Q] can split into many low-rank submatrix blocks, which can be low rank compression. In this paper, the multilevel UV method is applied to reduce the computational complexity and memory requirement of the BI part.

The multilevel UV method is a rank-based method. Generally, the interaction matrix is full-ranked when the observation groups are in the near field of the source group, while the interaction matrix between them is low-ranked when the observation groups are in the far field. Application of the UV decomposition to the low-ranked impedance matrix will result in significant memory and computational time savings. The basic principles of the UV decomposition can be found more detail in [21].

The whole object is divided into levels with the octree algorithm. Figure 1 illustrates a three level octree structure for a two-dimensional domain. The highest level has four blocks and the lowest level has $4l$ blocks where l is the number of levels. As proposed in [16], for the observation block (block 1) at level-1, the corresponding impedance matrix **Z**, which refers to the matrices [P] and [Q] in FE-BI, can be decomposed into l (l is the number of levels) sparse matrices,

$$\mathbf{Z}=\mathbf{Z}^0+\mathbf{Z}^1+\cdots+\mathbf{Z}^{l-1}, \tag{7}$$

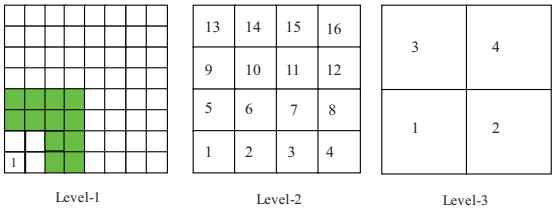

Fig. 1. A three level octree structure.

Since Z^0 is the near impedance matrix for the interactions of self and neighboring blocks at level-1, Z^0 is full-ranked and stored directly. Z^1 and so forth are the impedance matrices for the interactions of the far field, which is defined as the parent block's near field and the current block's far field. As shown in Fig. 1, the far field of block 1 at level-1 is the blocks 2, 5, and 6 at level-2 , since block 1 at level-2 is the parent block of block 1 at level-1 and the blocks 2, 5, and 6 are the neighbors of block 1 at level-2. Similarly, the far field of block 1 at level-1 is the region of blocks 3, 4, and 2 at level-3. The far field interactions are only evaluated at the peer level. The concept of the far field used above is

the same as it in the multilevel fast multipole algorithm (MLFMA) [16].

For Z^1 and so forth, the matrices are operated with two different ways according to their size, when applying the UV method. When the size of the matrix is small, it will be computed directly and its rank r is evaluated by singular value decomposition (SVD), then the **U** and **V** matrixes can be obtained. When the size of the matrix is large, the column and row sampling according to rank estimates is performed and SVD on the sampled matrix is implemented instead. So it should be noted that average ranks of the matrix blocks and the approximation precision increase by the decrease of truncation error. In the code, the rank of the first pair of groups is evaluated and the others are assumed the same as the first pair to further reduce the time for evaluating the rank. The above technique is feasible, since only the coarse estimation of the rank is needed in the UV algorithm [21]. The $m \times n$ matrix is then decomposed into **U**($m \times r$) and **V**($r \times n$) matrices, which leads to the significant time and memory savings when the matrix is low-ranked.

III. NUMERICAL RESULTS AND DISCUSSIONS

In this section, numerical examples are considered to demonstrate the accuracy and flexibility of our FE-BI algorithm for the analysis of electromagnetic scattering from arbitrary objects in half space. For the precision of the UV method. The truncation error of SVD is 1e-4 in the codes for these numerical examples. All numerical experiments are performed on a Pentium 4 with 2.9 GHz CPU and 2 GB RAM in double precision.

At first, Fig. 2 shows the bistatic scattering cross section of a bi-isotropic chiral sphere in the case of VV-polarizations. The chiral sphere is situated 40 cm above a lossy half space with a diameter of 0.6 m. The half space is characterized by ε_{gr} = 5.0 – j0.2 and σ_g = 0.01 S/m and at 300 MHz. The total number of unknowns is 45227 consisting of 40700 for the finite-element discretization and 4527 for BI. Two-level UV method is employed with the minimum group size 0.076 λ_0. The chiral body is assumed to have a relative chirality ξ_r and parameters $\varepsilon = \varepsilon_0\varepsilon_r / \left(1-\xi_r^2\right)$, $\mu = \mu_0\mu_r / \left(1-\xi_r^2\right)$, $\xi = -j\sqrt{\varepsilon\mu}\xi_r / \left(1-\xi_r^2\right)$, $\zeta = -\xi$, where $\varepsilon_r = 3.0$, $\mu_r = 1.0$ and $\xi_r = 0.3, 0.5, 0.8$. As shown in Fig. 2, the numerical results of the bistatic RCS is compared with those obtained by MoM [12]. It is obvious that an excellent agreement is obtained between them. Therefore, our algorithm has been proven to be accurate enough. The efficiency of the UV method for FE-BI solution is verified by comparing with the FE-BI without UV method. It takes 798.3 minutes to compute using FE-BI without UV method but only 265.2 minutes are need for the UV method. The memory requirement is 625.41 MB for BI part without UV method, but 211.38 MB for BI part with UV method.

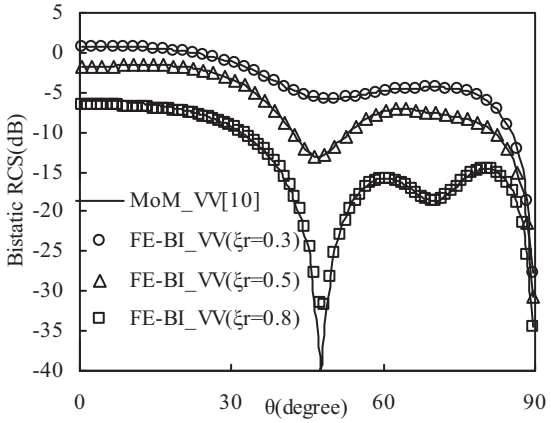

Fig. 2. Bistatic scattering cross section in the case of VV-polarization of a homogeneous chiral sphere above a lossy half space.

To validate our algorithm for computing the electromagnetic scattering of bi-anisotropic targets, the scattering cross section of a bi-anisotropic omega cylinder is computed and compared to the results in [10]. The bi-anisotropic omega media has constitutive tensors are in the form as follows,

$$\overline{\overline{\varepsilon}} = \varepsilon_0 \begin{bmatrix} \varepsilon_1 & 0 & 0 \\ 0 & \varepsilon_2 & 0 \\ 0 & 0 & \varepsilon_3 \end{bmatrix}, \quad \overline{\overline{\mu}} = \mu_0 \begin{bmatrix} \mu_1 & 0 & 0 \\ 0 & \mu_2 & 0 \\ 0 & 0 & \mu_3 \end{bmatrix}, \qquad (8)$$

$$\overline{\overline{\xi}} = \begin{bmatrix} 0 & 0 & 0 \\ -j\Omega & 0 & 0 \\ 0 & 0 & 0 \end{bmatrix}, \quad \overline{\overline{\zeta}} = \begin{bmatrix} 0 & j\Omega & 0 \\ 0 & 0 & 0 \\ 0 & 0 & 0 \end{bmatrix},$$

where $\varepsilon_1 = 2.0, \varepsilon_2 = 3.0, \varepsilon_3 = 2.0$, $\mu_1 = 1.2, \mu_2 = 1.2, \mu_3 = 1.0$ and Ω = 0.0, 0.5, and 1.0. Figures 3 and 4 show the bistatic scattering cross section of the finite omega cylinder in a free space, in the case of VV- and HH-polarizations [10]. The cylinder is meshed

into 4948 triangles and 34317 tetrahedrons. In Fig 3, the results obtained by our algorithm are in good agreement with those in [10].

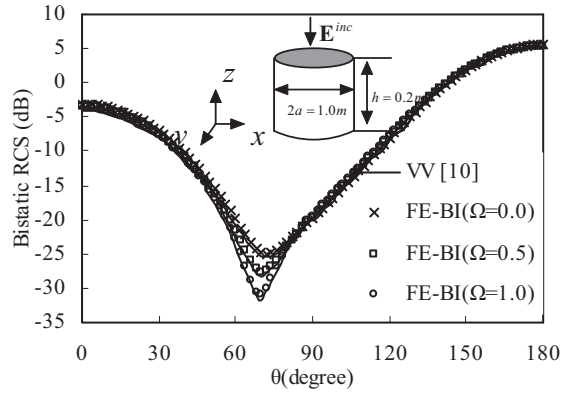

Fig. 3. Bistatic scattering cross section of a finite omega cylinder in free space in the case of VV-polarization.

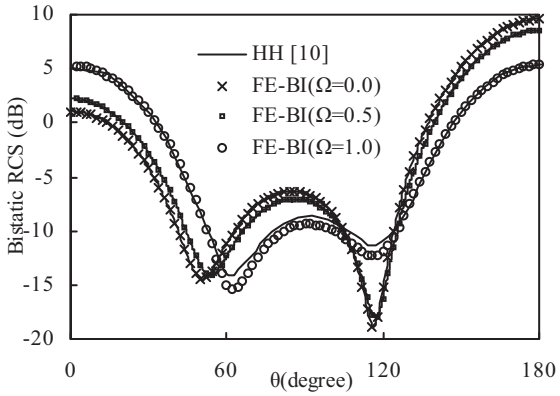

Fig. 4. Bistatic scattering cross section of a finite omega cylinder in free space in the case of HH-polarization.

Further, the bistatic scattering cross sections of the cylinder located at 0.3 m above a half space is studied via the FE-BI, as shown in Fig. 5. In the solution of FE-BI, two-level UV method is employed with the minimum group size 0.126 λ. The efficiency of the UV method for FE-BI solution is verified by comparing with the FE-BI without UV method. It takes more than 24 hours to compute using FE-BI without UV method but only 594.3 minutes are needed for the UV method. The memory requirement is 1.681 GB for BI part without UV method, but 387.28 MB for BI part with UV method.

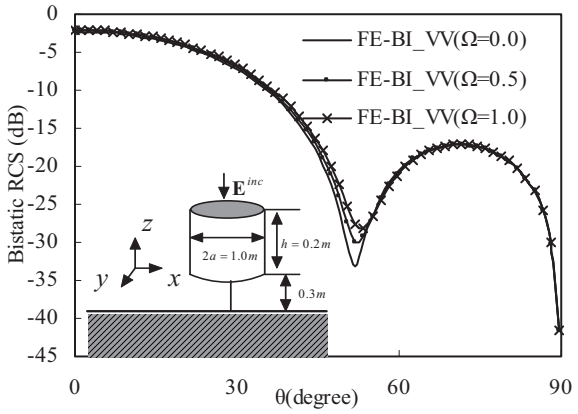

Fig. 5. Bistatic scattering cross section of a finite omega cylinder in half space in the case of VV-polarization.

Figure 5 at first shows the bistatic scattering cross section in the case of VV-polarization. It is shown that the Ω parameter has little effect on the scattering pattern in half space as well as in free space, shown in Fig. 3. As shown in Fig. 4, for the HH-polarization, the scattering pattern in free space can be modified effectively by the Ω parameter. However, as shown in Fig. 6, for the HH-polarization, the Ω parameter has less effect on the scattering pattern in half space than it has in free space. Moreover, it is interesting to note that the values of the HH-polarization RCS in free space increase with increasing magnitude of the Ω parameter, as observed in Fig. 4. However, the values of the HH-polarization RCS in half space slightly decrease with the increasing magnitude of the Ω parameter, as observed in Fig. 6. Of course, the scattering characteristics of a bi-anisotropic object depend on the combination of many different parameters, such as the four constitutive tensors, the incident wave form, the direction and polarization state etc. [10].

IV. CONCLUTION

In this paper, the FE-BI method has been developed for the analysis of electromagnetic scattering from arbitrary bi-anisotropic objects located above a lossy half space. The accuracy of the proposed method has been proven by comparison with published data. The multilevel UV method has been successfully applied to FE-BI to decrease the memory requirement and CPU time of solution. The effect of bi-anisotropic

parameters on the scattering characteristics is examined by considering the canonical examples. The present analysis shows that for VV-polarization scattering pattern, the bi-anisotropic parameters have less effect either in free space or half space. For HH-polarization scattering pattern, the bi-anisotropic parameters have great effect in free space, but it has actually little effect in free space in this analysis. Further, the present analysis may be useful in choosing appropriate bi-anisotropic materials to control the scattering characteristics in half space.

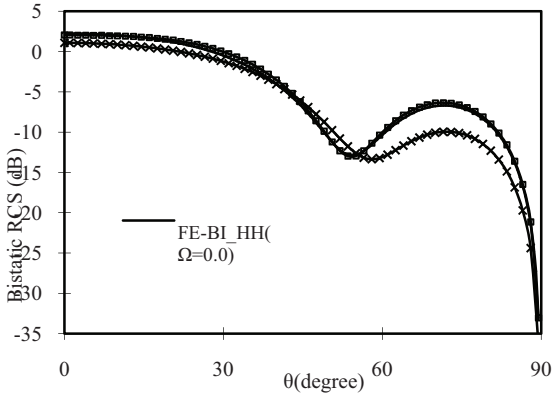

Fig. 6. Bistatic scattering cross section of a finite omega cylinder in half space in the case of HH-polarization.

ACKNOWLEDGMENT

This work was supported in part by Jiangsu Natural Science Foundation of BK2011757 and Jiangxi Natural Science Foundation of 20122BAB211018.

REFERENCES

[1] J. Volakis, A. Chatterjee, and L. Kempel, *Finite Element Method for Electromagnetics: Antennas, Microwave Circuits and Scattering Applications*, IEEE Press, New York, 1998.

[2] F.-G. Hu, C.-F. Wang, and Y.-B. Gan, "Efficient calculation of electromagnetic scattering from cavities coated with bianisotropic media using FE-BI method with higher-order tetrahedral elements," *IEEE Antennas and Propagation Society International Symposium*, pp. 3883-3886, July 2006.

[3] A. Semichaevsky, A. Akyurtlu, D. Kern, D. Werner, and M. Bray, "Novel BI-FDTD approach for the analysis of chiral cylinders and spheres," *IEEE Trans. Antennas Propag.*, vol. 54, no. 3, pp. 925-932, March 2006.

[4] F. Bilotti, L. Vegni, and A. Toscano, "Radiation and scattering features of patch antennas with bianisotropic substrates," *IEEE Trans. Antennas Propag.*, vol. 51, no. 3, pp. 449-456, March 2003.

[5] D. Wang, P. Lau, E. Yung, and R. Chen, "Scattering by conducting bodies coated with bi-isotropic materials," *IEEE Trans. Antennas Propag.*, vol. 55, no. 8, pp. 2313-2319, Aug. 2007.

[6] D. Worasawate, J. Mautz, and E. Arvas, "Electromagnetic scattering from an arbitrarily shaped three-dimensional homogeneous chiral body," *IEEE Trans. Antennas Propag.*, vol. 51, no. 5, pp. 1077-1084, 2003.

[7] I. Bogaert, "Accurate computation and tabulation of the scalar Green function for bi-anisotropic media and its derivatives," *28th Annual Review of Progress in Applied Computational Electromagnetics*, pp. 422-426, Columbus, Ohio, April 2012.

[8] X. Deng, C. Gu, and Y. Zhou, "Electromagnetic scattering by arbitrary shaped three-dimensional conducting objects covered with electromagnetic anisotropic materials," *Applied Computational Electromagnetics Society Journal*, vol. 26, no. 11, pp. 886-892, Nov. 2011.

[9] X. Yuan, D. Lynch, and J. Strohbehn, "Coupling of finite element and moment methods for electromagnetic scattering from inhomogeneous objects," *IEEE Trans. Antennas Propagat.*, vol. 38, pp. 386-393, March 1990.

[10] Y. Zhang, X. Wei, and E. Li, "Electromagnetic scattering from three-dimensional bianisotropic objects using hybrid finite element-boundary integral method," *J. of Electromagn. Waves and Appl.*, vol. 18, no. 11, pp. 1549-1563, 2004.

[11] S. Caorsi and R. Raffetto, "Perfectly matched layers for the truncation of finite-element meshes in layered half-space geometries and applications to electromagnetic scattering by buried objects," *Microwave Opt. Technol. Lett.*, vol. 19, no. 6, pp. 427-434, Dec. 1998.

[12] X. Wang, D. Werner, L.-W. Li, and Y.-B. Gan, "Interaction of electromagnetic waves with 3-D arbitrarily shaped homogeneous chiral targets in the presence of a lossy half space," *IEEE Trans. Antennas Propag.*, vol. 55, no. 12, Dec. 2007.

[13] R. Chen, Y. Hu, Z. Fan, D. Ding, D. Wang, and E. Yung, "An efficient surface integral equation solution to EM scattering by chiral objects above a lossy half space," *IEEE Trans. Antennas Propagt.*, vol. 57, no. 11, pp. 3586-3593, Nov. 2009.

[14] G. Pelosi, G. Toso, and R. Coccioli, "Finite-element boundry-integral analysis of electromagnetic scattering by a buried dielectric object," *Microwave and Optical Technology Letters*, vol. 24, no. 6, March 2000.

[15] D. Fang, J. Yang, and G. Delisle, "Discrete image theory for horizontal electric dipole in a multilayer medium," *Proc. Inst. Elect. Eng. H*, vol. 135, no. 5, pp. 297-303, Oct. 1988.
[16] W. Chew, J. Jin, E. Midielssen, and J. Song, *Fast and Efficient Algorithms in Computational Electromagnetics*, Boston, MA: Artech House 2001.
[17] Z. Liu, J. He, Y. Xie, A. Sullivan, and L. Carin, "Multilevel fast multipole algorithm for general targets on a half-space interface," *IEEE Trans. Antennas Propag.*, vol. 50, no. 12, pp. 1838- 1849, Dec. 2002.
[18] M. Li, H. Chen, C. Li, R. Chen, and C. Ong, "Hybrid UV/MLFMA analysis of scattering by PEC targets above a lossy half-space," *Applied Computational Electromagnetics Society Journal*, vol. 26, no. 1, pp. 17-25, Jan. 2011.
[19] D. Ding, J. Ge, and R. Chen, "Well-conditioned CFIE for scattering from dielectric coated conducting bodies above a half-space," *Applied Computational Electromagnetics Society Journal*, vol. 25, no. 11, pp. 936-946, Nov. 2010.
[20] L. Felsen and N. Marcuvitz, *Radiation and Scattering of Waves Piscataway*, NJ: IEEE Press ch. 4, 1996.
[21] L. Tsang, Q. Li, P. Xu, D. Chen, and V. Jandhyala, "Wave scattering with UV multilevel partitioning method: 2. Three-dimensional problem of nonpenetrable surface scattering," *Radio Sci.*, vol. 39, pp. RS5011, 2004.
[22] S. Rao, D. Wilton, and A. Glisson, "Electromagnetic scattering by surfaces of arbitrary shape," *IEEE Trans. Antennas Propag.*, vol. 30, pp. 409-418, 1982.
[23] J. Jin, *The Finite Element Method i n Electromagnetics. 2nd ed.,* New York: John Wiley & Sons, Inc., 2002.

Jian Zhu received the B.S. and Ph.D degrees in electromagnetic fields and microwave technology from Nanjing University of Science and Technology (NUST), China, in 2004 and 2010, respectively.
She is currently a lecturer of Nanjing University of Posts and Telecommunications. Her current research interests include CEM and antennas.

Meng-Meng Li was born in Jiangsu Province, the People's Republic of China in 1984. He received B.S. degree in physics from Huaiyin normal college in 2007, and is currently working toward the PH.D. degree at Nanjing University of Science and Technology. His research interests focus on fast solution of integral equations, modeling of microwave integrated circuits and UWB antennas.
Mr Li received the student paper award from the 2012 International Conference on Microwave and Millimeter Wave Technology.

Z. H. Fan was born in Jiangsu, China, in 1978. He received the M.Sc and Ph.D degrees in electromagnetic field and microwave technique from Nanjing University of Science and Technology (NJUST), Nanjing, China, in 2003 and 2007, respectively. During 2006, he was with the Center of wireless Communication in the City University of Hong Kong, Kowloon, as a Research Assistant. He is currently a Lecturer with the Electronic Engineering of NJUST. He is the author or coauthor of over 20 technical papers. His current research interests include computational electromagnetics, electromagnetic scattering and radiation.

Ru-shan Chen received the B.S. and M.S. degrees in electronic from Southeast University, China, in 1987 and 1990, respectively, and the Ph.D. degree from the Department of Electronic Engineering, City University of Hong Kong (CUHK), Hong Kong SAR, China, in 2001. In 1990, he joined the Department of Electronic Engineering, Nanjing University of Science and Technology (NUST), China. Since 1996, he has been a Visiting Scholar with the Department of Electronic Engineering, CUHK. In 1999, he was promoted Full Professor of NUST, and in 2007, he was appointed Head of the Department of Communication Engineering.
His research interests mainly include CEM and millimeter wave systems. He has authored or coauthored more than 200 papers, including over 140 papers in international journals. Dr. Chen is the recipient of the Foundation for China Distinguished Young Investigators in 2003. In 2008, he became a Chang-Jiang Professor under the Cheung Kong Scholar Program of China.